Solution mechanisms of phosphorus in quenched hydrous and anhydrous granitic glass as a function of peraluminosity

B. O. Mysen, Holtz François, Michel Pichavant, Jean-Michel Bény, J.M. Montel

Pergamon

Geochimica et Cosmochimica Acta, Vol. 61, No. 18, pp. 3913–3926, 1997

0016-7037/97 $17.00 + .00

PII S0016-7037(97)00193-2

Solution mechanisms of phosphorus in quenched hydrous and anhydrous granitic glass as a function of peraluminosity

B. O. MYSEN,[1] F. HOLTZ,[2,*] M. PICHAVANT,[2] J.-M. BENY,[2] and J.-M. MONTEL[3]

[1]Geophysical Laboratory and Center for High Pressure Research, Carnegie Instn. Washington, 5251 Broad Branch Rd., NW., Washington, DC 20015, USA
[2]CRSCM-CNRS, 1a, rue de la Ferollerie, 45071 Orleans, France
[3]Department de Geologie, URA 10 du CNRS, Universite Blaise Pascal, 5, rue Kessler, 63038 Clermont-Ferrand, France

(*Received June* 21, 1996; *accepted in revised form May* 16, 1997)

Abstract—Solution mechanisms of P in metaluminous to peraluminous quenched, hydrous (~9 wt% H_2O) and anhydrous glasses in the system CaO-Na_2O-K_2O-Al_2O_3-SiO_2-P_2O_5 have been examined with microRaman spectroscopy. The principal aim was to examine relative stability of phosphate complexes as a function of bulk chemical composition. Increasing peraluminosity was accomplished by increasing Al^{3+} and Ca^{2+} proportions with constant SiO_2 content. The molar ratio $Al_2O_3/(CaO + Na_2O + K_2O)$(A/CNK) ranged from 1 (metaluminous) to ~1.3 (peraluminous).

In all compositions P^{5+} is bonded to Al^{3+} to form $AlPO_4$ complexes. The principal solution mechanism is one where depolymerized species (Q^3), involving Al^{3+} both within and outside the aluminosilicate network, interact with P to form the $AlPO_4$ complex together with Q^4 species. The mechanism does not involve alkali metals or alkaline earths. In anhydrous compositions, the spectra are interpreted to suggest Si-O-P cross-linking in the structure. In hydrous compositions, evidence for Si-O-P bonding is less evident. In such glasses, there is, however, possible spectroscopic evidence for Si-OH bonding and possibly P-OH bonding resulting from breakage of cross-linking Si-O-P bonds existing in the anhydrous glasses. Therefore, the water content of peraluminous aluminosilicate melts is likely to affect the solubility behavior of P, and conversely, the solubility behavior of H_2O is affected by P in such melts.

1. INTRODUCTION

The geochemical behavior of phosphorus in both mafic and silicic magmas is receiving increasingly detailed attention (e.g., Ryerson and Hess, 1980; Watson and Capobianco, 1981; Harrison and Watson, 1984; Pichavant et al., 1992; Toplis et al., 1994a,b; Wolf and London, 1994). Although generally present in comparatively low concentrations in natural magmas (less than 2–3 wt% P_2O_5), even in this abundance range P strongly modifies both physical and chemical properties of silicate liquids (Wyllie and Tuttle, 1964; Kushiro, 1975; Watson, 1976; Visser and Koster Van Groos, 1979; Ryerson and Hess, 1980; London, 1987; Dingwell et al., 1993; London et al., 1993; Toplis et al., 1994a; Toplis and Dingwell, 1996).

In silicic magmas, the P concentration generally is buffered by the solubility of apatite. Early studies (Ryerson and Hess, 1980; Watson and Capobianco, 1981; Harrison and Watson, 1984) have determined that apatite solubility in felsic melts is dependent primarily on temperature and melt SiO_2 content and generally is small for crustal temperatures and melt compositions (e.g., 0.02 wt% P_2O_5 for a melt having 75 wt% SiO_2 at 800°C, Harrison and Watson, 1984). Recent studies, however, have revealed that apatite solubility depends in a complex way on other melt compositional parameters such as the balance between Al and alkali plus Ca (i.e., A/CNK = $Al_2O_3/(CaO + Na_2O + K_2O)$, molar (Pichavant et al., 1992; Richard et al., 1992; Wolf and London, 1994), and FeO/Fe_2O_3 ratio (Richard et al., 1992). For constant melt SiO_2 content and temperature, apatite solubility is increased dramatically for peraluminous liquids (A/CNK > 1). Solubilities of up to several wt% P_2O_5 for peraluminous silicic liquids in equilibrium with apatite at 750–1000°C have been reported (Pichavant et al., 1992; Richard et al., 1992; Wolf and London, 1994). To be interpreted, such results require a better understanding of the structural role of P with the aid of detailed structural studies of multicomponent P-bearing aluminosilicate melt compositions.

Most P-bearing silicate melt compositions studied in the glass literature are peralkaline, i.e., molar contents of alkali greatly exceeds that of Al (A/CNK < 1). For such compositions, results of spectroscopic studies have shown that the addition of P increases polymerization of silicate network. In those melts alkali metals associate with P to form phosphate complexes and the number of nonbridging oxygens decreases (Nelson and Tallant, 1984; Dupree et al., 1988, 1989). In contrast, for both subaluminous (A/CNK = 1) and peraluminous (A/CNK > 1) melts, it has been suggested that P speciation is characterized by the presence of $AlPO_4$-like units (Mysen et al., 1981; Kosinski et al., 1988; Dupree et al., 1989; Gan and Hess, 1992). Complexing of P^{5+} with Al^{3+} in peraluminous aluminosilicate melts would account for the strong increase of apatite solubility found experimentally (Pichavant et al., 1992; Wolf and London, 1994). However, none of the different spectroscopic studies

* *Present address:* Inst. Mineralogie, Univ. Hannover, Welfengarten 1, D-30167 Hannover, Germany.

Table 1. Composition of the glasses.

	244			245			246			247		
	nom	wet	dry	nom	wet	dry	nom	wet	dry	nom	wet	dry
SiO_2	75.00	69.06	75.97	75.00	68.54	75.79	75.00	65.79	74.89	75.00	69.32	75.50
Al_2O_3	14.10	12.62	13.88	14.40	12.85	14.21	14.70	12.72	14.48	14.80	13.96	15.11
CaO	0.21	0.19	0.21	1.47	1.32	1.46	2.73	2.55	2.90	4.00	3.07	3.32
Na_2O	4.18	3.56	3.92	3.18	2.68	2.96	2.20	1.92	2.19	1.26	1.50	1.62
K_2O	6.35	5.35	5.89	4.83	4.04	4.47	3.30	2.88	3.28	1.91	2.16	2.34
P_2O_5	0.16	0.12	0.13	0.12	1.00	1.11	2.07	1.99	2.27	3.03	2.36	2.55
Total	100.00	90.90	100.00	100.00	90.43	100.00	100.00	87.85	100.00	100.00	92.37	100.00
A/CKN*	1.01	1.07	1.07	1.22	1.29	1.29	1.51	1.48	1.48	1.91	1.84	1.84
Na/K**	1.00	1.01	1.01	1.00	1.10	1.01	1.00	1.01	1.01	1.00	1.06	1.06
Ca/P**	1.66	2.00	2.00	1.66	1.67	1.67	1.67	1.62	1.62	1.67	1.65	1.65
	248			249			250			251		
	nom	wet	dry	nom	wet	dry	nom	wet	dry	nom	wet	dry
SiO_2	75.00	67.75	75.69	75.00	68.03	75.92	75.00	68.96	75.56	75.00	67.92	75.48
Al_2O_3	14.10	12.47	13.93	14.30	12.58	14.04	14.40	12.83	14.06	14.40	12.88	14.31
CaO	0.12	0.08	0.09	0.88	0.79	0.88	1.64	1.49	1.63	2.40	2.10	2.33
Na_2O	4.21	3.51	3.92	3.46	2.83	3.16	2.74	2.41	2.64	2.05	1.79	1.99
K_2O	6.41	5.57	6.22	5.24	4.41	4.92	4.16	3.54	3.88	3.11	2.73	3.03
P_2O_5	0.16	0.13	0.15	0.12	0.97	1.08	2.06	2.04	2.24	3.04	2.57	2.86
Total	100.00	89.51	100.00	100.00	89.61	100.00	100.00	91.27	100.00	100.00	89.99	100.00
A/CKN*	1.01	1.05	1.05	1.17	1.24	1.24	1.37	1.40	1.40	1.61	1.65	1.65
Na/K**	1.00	0.96	0.96	1.00	0.98	0.98	1.00	1.03	1.03	1.00	1.00	1.00
Ca/P**	0.95	0.78	0.78	0.99	1.03	1.03	1.00	0.92	0.92	1.00	1.03	1.03

* Molar ratio, $Al_2O_3/(CaO + Na_2O + K_2O)$ **Atomic ratios

so far available have been conducted on compositions approaching either natural peraluminous or experimental melts showing elevated apatite solubility.

Here, we present room temperature Raman spectroscopic data on the mechanisms of solution of P_2O_5 in peraluminous quenched melts (glass) in the system SiO_2-Al_2O_3-Na_2O-K_2O-CaO-P_2O_5 with and without H_2O. The data concern two series of glasses, one with a Ca/P ratio of 5/3 (i.e., same as in apatite) and the other with Ca/P = 1, thus enabling to test the possible preference of P to coordinate with Ca rather than with Al.

2. EXPERIMENTAL AND ANALYTICAL METHODS

2.1. Preparation of Glasses

Starting materials were P_2O_5-free gels (or glasses). Nominally, these have constant SiO_2 content of 75 wt% and constant Na/K of 1. In each series of four compositions (1: Ca/P = 5/3 and 2: Ca/P = 1), Al and Ca progressively increase (along with P concentration), whereas the total alkali contents decrease, resulting in compositions becoming progressively more peraluminous (A/CNK = 1.0, 1.1, 1.2, 1.3, Table 1). There is, therefore, a positive correlation between A/CNK and phosphorus content of the two series of glasses (Fig. 1).

The glasses were initially synthesized hydrous at high pressure and temperature. The source of P_2O_5 was an H_3PO_4 solution. The gels were loaded in Pt capsules, together with the H_3PO_4 solution and a small additional amount of demineralized doubly-distilled water added so that glasses contain 9–10 wt% H_2O. Two batches of eight hydrous glasses (about 200 mg each) were synthesized in internally-heated pressure vessels, respectively, at 1100°C, 8 kbar for 7–9 days (see description of apparatus by Vielzeuf and Montel, 1994), and 1300°C, 4 kbar for 3 days (see Roux et al., 1994, for description of apparatus).* The samples were contained in sealed Pt containers.

All glasses were analyzed with a Cameca SX 50 electron microprobe to check for their composition and chemical homogeneity. Analytical conditions and standards were those established previously for P_2O_5-bearing glasses of similar compositions (Pichavant et al., 1992) using the precautions described by Pichavant (1987) for analysis of hydrous alkali aluminosilicate glasses. Results are given in Table 1 and recalculated to 100% to compare with nominal compositions. Macusani glass was used as P_2O_5 standard. The water contents of two of the glasses, 245 and 248, were determined with Karl Fischer titration (Behrens, 1995; Holtz et al., 1995). The analyzed values (8.53 and 8.27 wt% H_2O, respectively) compare well with the maximum water contents from the proportions of the reactants (8.9–9.1 wt%).

The Raman microspectroscopic analyses of the dry compositions were performed from small chips of hydrous glasses that were slowly dehydrated in situ in a Pt wire furnace of the type developed by Mysen and Frantz (1992) for high-temperature, in situ microRaman spectroscopy. Complete dehydration was taken as that where there was no longer Raman intensity near 3600 cm^{-1} (OH stretching) corresponding to less than 0.1 wt% H_2O in the glass (B. O. Mysen and D. Virgo, unpubl. data). The Raman analyses of hydrous glasses were carried out on small glass chips.

Raman spectra were recorded with a Dilor XY confocal microRaman spectrometer equipped with a cryogenic Wright Model CCD

* All samples except no. 246 were prepared at 1100°C and 8 kbar. Sample 246 was prepared at 1300°C and 4 kbar.

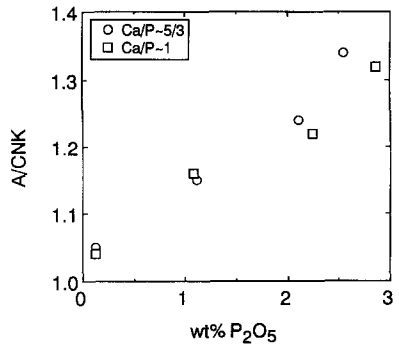

Fig. 1. Relationship between peraluminisity (A/CNK) and P_2O_5 content of the glasses.

05-11-0-202 charge-coupled detector (CCD). The excitation source was the 514 nm line of a Coherent Innova Model 90-5 Ar^+ laser operating at several hundred mW at the sample. Integration times ranged from 60 to 300 s. The spectra were recorded in the frequency ranges 200–1800 cm^{-1} and 3000–4000 cm^{-1}.

The high-frequency portion of the spectra was deconvoluted with lines of Gaussian shape as is normally done with Raman spectra of silicate glasses (See Mysen, 1992, for detailed discussion). Prior to deconvolution of the spectra, the instrumental background was subtracted by using a line obtained by least-square fitting of the data points at frequencies where no Raman scattering was observed. The spectra were then corrected for temperature- and frequency-dependent scattering intensity (Long, 1977) and the intensities were normalized to the absolute maximum intensity. The curve-fitting is based on the minimization of the squares of the deviations between the observed and calculated Raman envelopes using the algorithm described by Davidon (1966) (see also Seifert et al., 1982; Mysen et al., 1982; Mysen, 1992, for details). The line parameters were treated as independent variables. The number of lines was determined statistically to be that number where additional lines did not improve the quality of the fit significantly. A significant shift in χ^2 corresponds to a 10% or more improvement when increasing the number of independent variables by (Hamilton, 1965). As three independent variables are needed to describe one line, a 10% improvement in χ^2 is required to justify an increase in the number of fitted lines by one.

3. RESULTS

The Raman spectra can be divided into two frequency regions. The low-frequency region between 200 and 1300 cm^{-1} contains the first order Raman bands associated with the aluminosilicate network (see Fig. 2 for examples). That between 3000 and 4000 cm^{-1} contains the O-H stretch vibrations from hydroxyl groups and molecular H_2O in samples containing dissolved H_2O (Fig. 3). The presence of molecular H_2O in the glass samples is evidenced by the weak band near 1600 cm^{-1} assigned H-O-H bending.

3.1. Low-Frequency Region (200–1300 cm^{-1})

The Raman spectra of anhydrous glasses (e.g., Fig. 2) overall show similar topology with a broad band centered near 1100 cm^{-1}. This maximum is asymmetric toward lower frequency. There is another strong maximum near 500 cm^{-1} with additional spectral detail near 600 cm^{-1}. There is also a distinctive band near 800 cm^{-1}. The overall topological

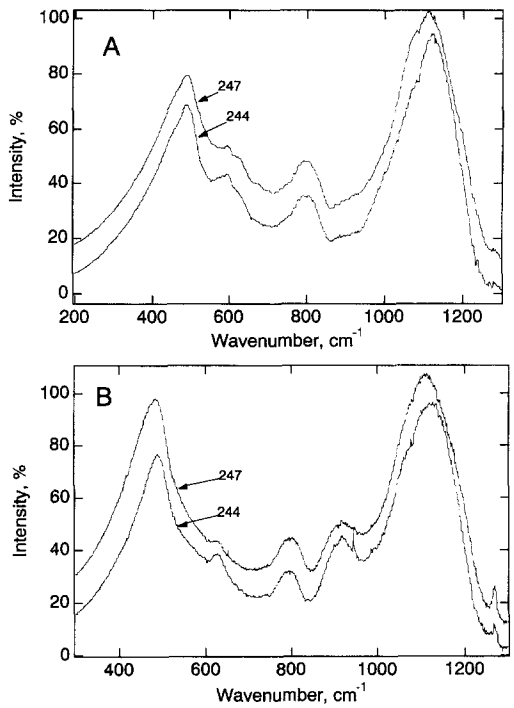

Fig. 2. Examples of unpolarized Raman spectra in the low-frequency region of nominally P-free (244) and P-bearing (247) glasses anhydrous (A) and hydrous (B).

features resemble those of other highly polymerized aluminosilicate glasses (e.g., McMillan et al., 1982; Seifert et al., 1982; Matson et al., 1986).

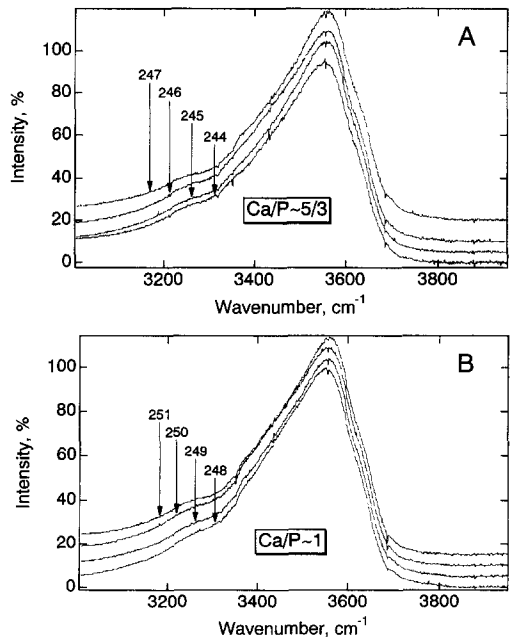

Fig. 3. Unpolarized Raman spectra in the spectral region of OH stretching.

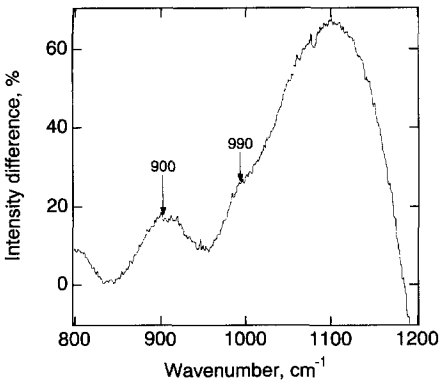

Fig. 4. Difference spectra (hydrous-anhydrous) in the 800–1200 cm^{-1} range illustrating the influence of H_2O on the Raman intensities. Sample 244 is nominally P-free.

In the 200–1300 cm^{-1} region, the principal spectral effect resulting from added H_2O to the samples is the appearance of a broad strong band near 900 cm^{-1} (Fig. 2), an observation consistent with those of Mysen and Virgo (1986a) and McMillan et al. (1993). In both the P-free and P-bearing samples, the difference spectra (hydrous–anhydrous samples) also reveal a shoulder near 990 cm^{-1} (Fig. 4).

Addition of phosphorus to both hydrous and anhydrous samples, whether at Ca/P ~ 5/3 or Ca/P ~ 1, results only in subtle spectral changes (Fig. 2a, cf. spectrum 244, which is nominally P-free, and spectrum 247, which contains nearly 3 wt% P_2O_5). There appears to be a shoulder slightly below 1100 cm^{-1}, a feature more clearly shown as a maximum near 1070 cm^{-1} in the difference spectra (P-bearing–P-free; see Fig. 5). In anhydrous samples with the highest Ca/P (~5/3; samples 245–247), a subtle intensity increase near 940 cm^{-1} with increasing phosphorus content may also be discerned (Fig. 5d). This latter effect is less clear in the samples with Ca/P ~ 1 (samples 249–251; Fig. 5c). In the spectra of the hydrous glasses (Fig. 5a,b), this latter effect is obscured by the significant intensity increase near 970–990 cm^{-1} (see also Fig. 4). These spectral changes near 940 and 1100 cm^{-1} are qualitatively analogous to those of other P-bearing aluminosilicate glasses (e.g., Gan and Hess, 1992). The presence of phosphorus in the glasses also results in an intensity increase in the Raman spectra of such samples near 1210–1220 cm^{-1} (marked as 1210 in Fig. 5).

The spectra of P-bearing, hydrous samples (see Fig. 2b, for example) show the same overall topological features as the spectra of P-free hydrous samples. It is evident, however, that the intensity near 900 cm^{-1} diminishes with increasing P-content (and concomitant increase in peraluminosity; see Fig. 5a,b).† Increasing P-content also results in enhanced intensity near 1070 cm^{-1} for the Ca/P ~ 1 series. This intensity change is less pronounced for hydrous samples with Ca/P ~ 5/3 (Fig. 5a,b).

† This effect appears as an increasingly deep valley in the difference spectra in Fig. 5A,B.

3.1.1. Curve-fitted spectra

The spectral region between ~850 and 1250 cm^{-1} was fitted to Gaussian bands with the number of bands statistically determined as described above (experimental methods). Typical examples are shown in Fig. 6. A summary of the frequencies and areas of these bands is given in Table 2.

The spectra of P-free, anhydrous glasses were fitted to a very weak band near 900 cm^{-1}, and three strong bands near 1000, 1100, and 1200 cm^{-1}, respectively, similar to other Raman data from highly polymerized aluminosilicate glasses (e.g., Seifert et al., 1982).‡ For the anhydrous, P-bearing samples, the frequencies of the latter three bands are only very subtly dependent on the phosphorus content (Table 2). In the spectra of hydrous, both P-free and P-bearing samples, the frequencies of these latter three bands are distinctly higher (by as much as 20–30 cm^{-1}) than in the spectra of the equivalent anhydrous samples. This observation accords with other spectroscopic data on the effect of H_2O content on Raman frequencies in this frequency range for aluminosilicate glasses (Mysen and Virgo, 1986a).

In the presence of H_2O (e.g., Fig. 6b,d; see also Tables 2 and 3 for complete set of data), a strong band occurs near 900 cm^{-1} in accord with other Raman and infrared spectroscopic data of hydrous aluminosilicate glasses (e.g., Mysen et al., 1980; Remmele et al., 1986; Mysen and Virgo, 1986a,b; Silver and Stolper, 1989; McMillan et al., 1993; Holtz et al., 1996). A band near 970 cm^{-1} is also observed (Fig. 6, see also Table 2). In the spectra of P-containing glasses, whether hydrous or anhydrous, two additional bands near 1100 and 1210 cm^{-1}, respectively, are needed to satisfy the spectral envelope (e.g., Fig. 6). In the hydrous, phosphorus-bearing samples, a band near 940 cm^{-1} could also be fitted. This band is less evident in spectra of anhydrous, P-bearing samples (Table 3). In all cases, whenever present the frequencies of the 940, 1100, and 1210 cm^{-1} bands appear insensitive to H_2O and P concentrations (Table 2).

3.2. High-Frequency Region (3000–4000 cm^{-1})

The high-frequency region between 3000 and 4000 cm^{-1} of the spectra of all the hydrous samples is quite similar (Fig. 3) with a broad intensity maximum near 3600 cm^{-1}, asymmetric toward lower frequencies and with a small shoulder near ~3300 cm^{-1}. This spectral topology is similar to that of other hydrous, highly polymerized aluminosilicate glasses (e.g., Mysen et al., 1980; Mysen and Virgo, 1986a,b; McMillan et al., 1993).

3.2.1. Curve-fitted spectra

In the curve-fitted spectra, four Gaussian bands near 3300, 3500, 3600, and 3650 cm^{-1} were inserted (Fig. 7). Their

‡ The anhydrous, P-free glasses (no. 244 and 248; see Table 1) have NBO/T values of 0.022 and 0.027, respectively. Thus any contribution from nonbridging oxygen is not likely to be detected in the Raman spectra.

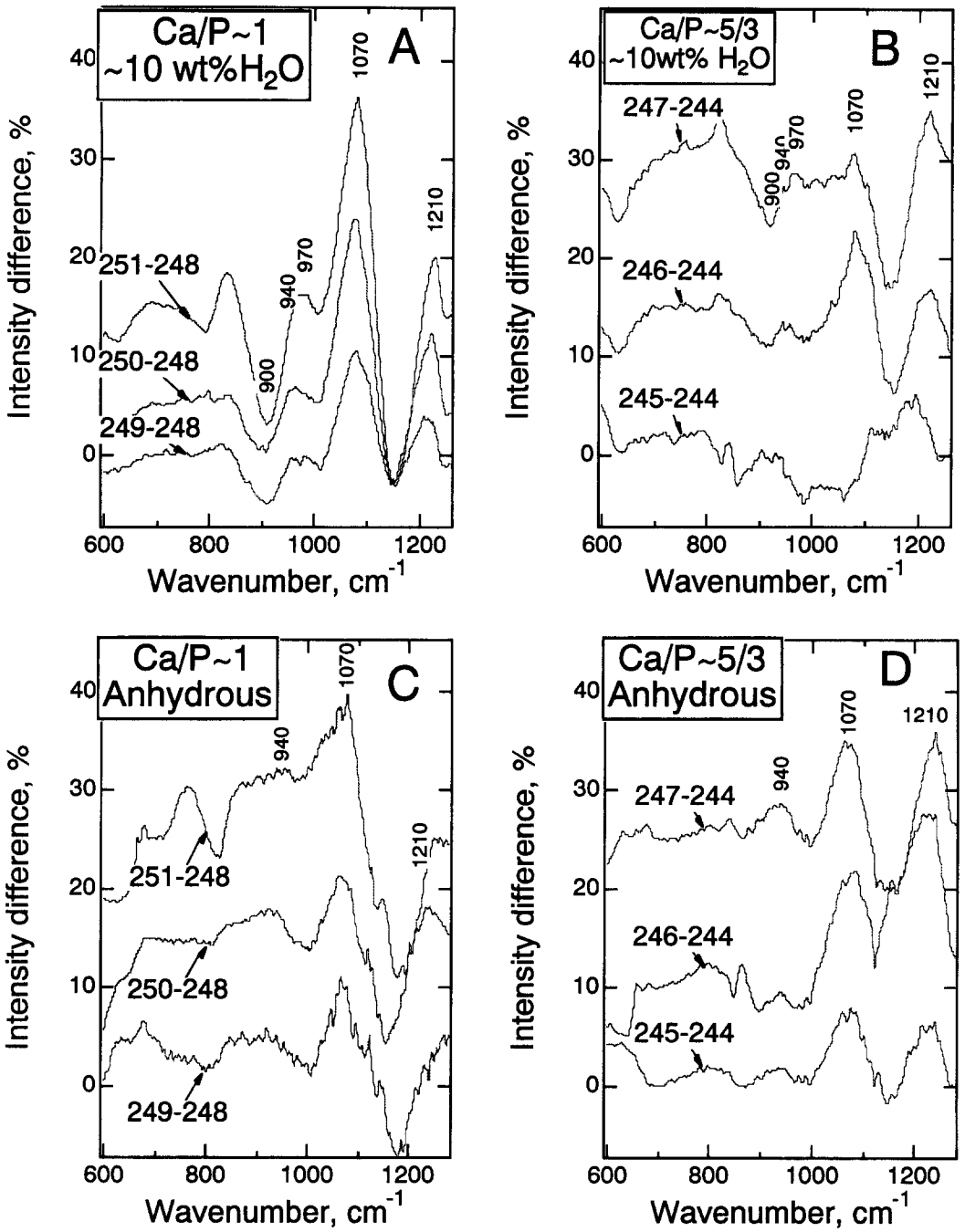

Fig. 5. Difference spectra illustrating the effect of increased phosphorus content for the two series of samples both anhydrous and hydrous. (A) The series Ca/P ~ 1 with approximately 10 wt% H_2O in solution. The spectra 249, 250, and 251 were subtracted from spectrum 248 (nominally P-free). (B) As A, but for the series Ca/P ~ 5/3. In this series spectra 245, 246, and 247, were subtracted from the nominally P-free spectrum 244. (C) As A, but for anhydrous samples. (D) As B, but for anhydrous samples.

frequencies, with the exception of the band near 3300 cm^{-1}, are insensitive to Ca/P, A/CNK, and phosphorus content (Table 4). The lowest-frequency band, near 3300 cm^{-1}, exhibits a slight frequency decrease as the phosphorus content is increased (Table 4). The relative band areas vary systematically with P_2O_5 content (Fig. 8). Notably, in the Ca/P ~ 5/3 series, the band near 3500 cm^{-1} grows and those near 3300 and 3600 cm^{-1} diminish, whereas the opposite trends with P-content is observed in the spectra of the Ca/P ~ 1 series of glasses (Fig. 8). The band near 3650 cm^{-1} is quite weak in all spectra ranging in relative area from 1.3 to 2.2% of the total area of the envelope.

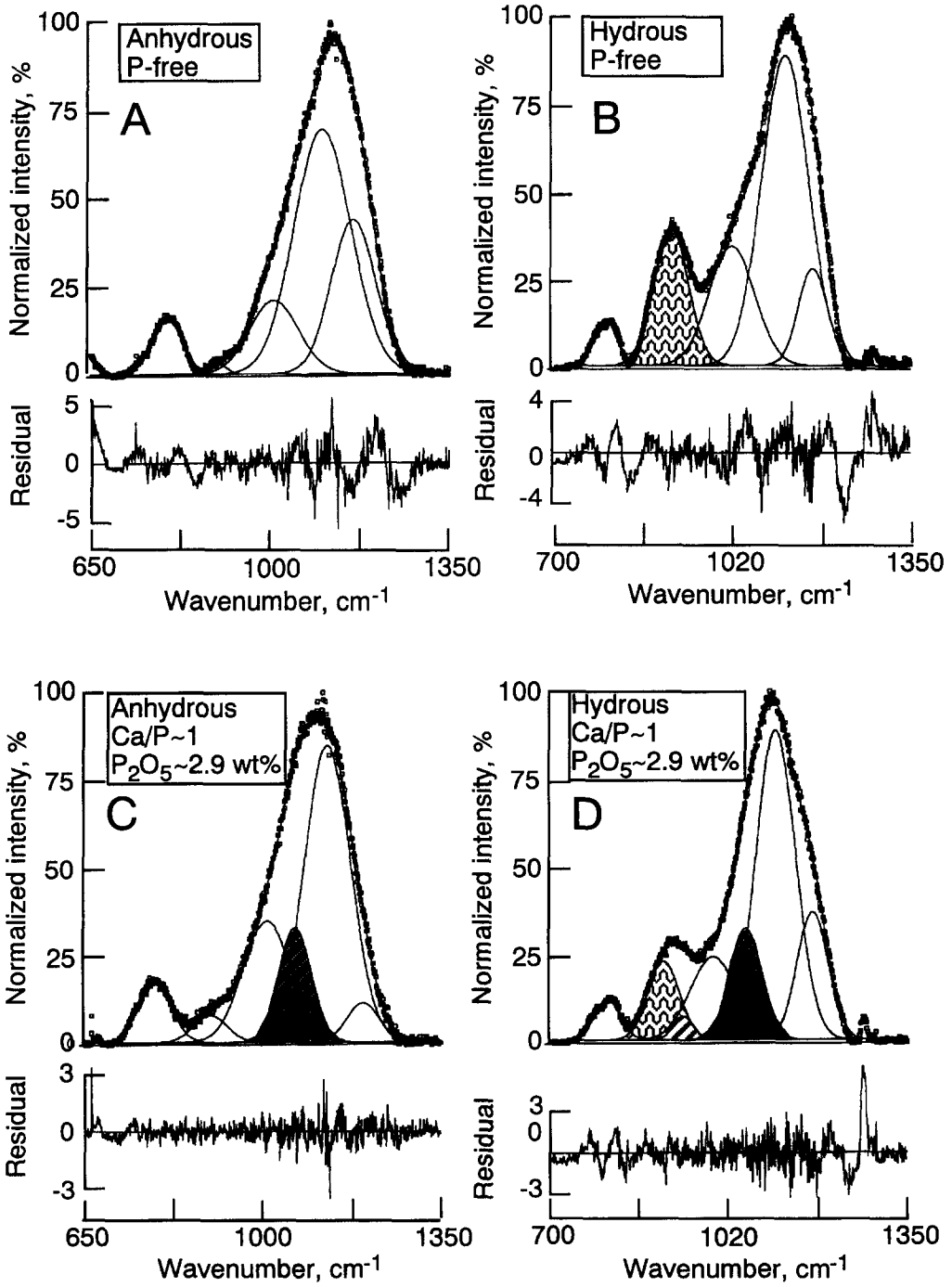

Fig. 6. Examples of curve-fitted spectra. Bands assigned to vibrations resulting from the presence of H_2O are shown with dotted patterns, whereas bands assigned to vibrations associated with phosphorus are indicated with hachured patterns.

3.3. Band Assignments and Structural Interpretation

The starting point for interpretation of the aluminosilicate glass spectra is that of vitreous SiO_2 where two average structures differing in the number of tetrahedra in the three-dimensionally interconnected rings are commonly suggested (Mammone et al., 1981; Galeener, 1982; Seifert et al., 1982, 1983; Revesz and Walrafen, 1983). These two ring structures give rise, for example, to the two bands near 1150 and 1200 cm^{-1} both of which are assigned to Si-O° stretch vibrations. A detailed analysis of spectra of glasses along the join SiO_2-$NaAlO_2$ led Seifert et al. (1982) to conclude

Table 2. Experimental results—line parameters in 700–1300 cm^{-1} region.

		Frequency							
wt% P_2O_5	Al/(Al + Ca + Na)	900	940	970	1000	1110	1100	1200	1210
Ca/P~5/3									
Anhydrous									
0.13	1.05	901			1000		1092	1160	
1.11	1.15	912			996	1119	1080	1158	1205
2.11	1.24		938		994	1117	1077	1154	1205
2.55	1.34		938		990	1118	1073	1151	1211
~10 wt% H_2O									
0.13	1.05	912		976	1045		1124	1180	
1.11	1.15	907	939	970	1043	1121	1112	1173	1211
2.11	1.24	907	940	977	1037	1123	1102	1173	1212
2.55	1.34	906	939	976	1036	1123	1102	1175	1211
Ca/P~1									
Anhydrous									
0.15	1.04	900			1002		1092	1160	
1.08	1.16	910			997	1118	1080	1154	1205
2.24	1.22	915			995	1120	1079	1154	1206
2.86	1.32	906			997	1116	1078	1154	1205
~10 wt% H_2O									
0.15	1.04	912		968	1046		1126	1178	
1.08	1.16	904	938	974	1042	1122	1109	1173	1211
2.24	1.22	904	937	971	1040	1124	1102	1172	1210
2.86	1.32	906	937	977	1038	1122	1101	1172	1210

		Areas															
wt% P_2O_5	Al/(Ca + Na + K)	900	±1σ	940	±1σ	970	±1σ	1000	±1σ	1100	±1σ	1100	±1σ	1200	±1σ	1210	±1σ
Ca/P~5/3																	
Anhydrous																	
0.13	1.05	50	21					1027	104			4683	285	3266	248		
1.11	1.15	92	28					1066	69	880	50	4232	129	2121	102	1169	71
2.11	1.24			27	19			654	65	785	78	4566	120	2371	208	1859	146
2.55	1.34			303	49			506	57	235	30	4339	116	3197	76	874	42
~10 wt% H_2O																	
0.13	1.05	941	48			870	60	1299	60			6546	118	471	41		
1.11	1.15	745	35	223	38	499	84	1527	145	496	64	4349	175	1912	89	52	17
2.11	1.24	740	60	283	99	467	201	1121	329	418	240	5042	485	1683	225	224	83
2.55	1.34	583	50	253	85	609	98	1039	78	421	209	4986	299	2001	62	153	32
Ca/P~1																	
Anhydrous																	
0.15	1.04	80	29					1182	98			4691	158	3756	127		
1.08	1.16	139	33					1110	116	515	41	4170	196	2439	115	1038	70
2.24	1.22	288	46					911	55	377	30	4366	102	2457	78	1026	61
2.86	1.32	115	31					1343	111	793	103	4291	198	2341	94	641	70
~10 wt% H_2O																	
0.15	1.04	1281	70			819	66	1820	49			4753	99	1107	52		
1.08	1.16	757	38	384	54	547	80	1348	80	829	66	4091	109	1713	61	27	10
2.24	1.22	812	47	443	36	457	50	1473	313	629	255	4503	632	1681	398	170	106
2.86	1.32	570	37	367	61	572	121	1000	224	410	171	4852	403	1383	124	172	103

Table 3. Area of 940 cm^{-1} band relative to total area# of high-frequency envelope (850–1300 cm^{-1}).

Wt% P_2O_5	A/CNK*	Hydrous ($\pm 1\sigma$)	Anhydrous ($\pm 1\sigma$)
Ca/P~5/3			
1.11	1.15	0.024 (4)	n.d.
2.11	1.24	0.030 (10)	0.003 (2)
2.55	1.34	0.027 (9)	0.004 (5)
Ca/P~1			
1.08	1.15	0.042 (6)	n.d.
2.24	1.24	0.046 (4)	n.d.
2.86	1.34	0.042 (7)	n.d.

The area of the 970 cm^{-1} band not included.
n.d. Not Detected.
* Molar $Al_2O_3/(CaO + Na_2O + K_2O)$.

that a similar structural environment existed as Al^{3+} substituted for Si^{4+} in glasses along this join. The frequencies of the bands near 1150 and 1200 cm^{-1} in spectra of vitreous SiO_2 decreased systematically with increasing Al/(Al + Si). In the present spectra of anhydrous, P-free glasses, bands assigned to (Si,Al)-O° stretching, occur near 1090 and 1160 cm^{-1}, respectively (Table 2; see also Fig. 6a).

The assignment of the ~900 cm^{-1} band in spectra of all hydrous samples (whether P-bearing or nominally P-free) as well as in published spectra of other hydrous aluminosilicate glasses has been the subject of debate. One assignment is to (Si,Al)-OH stretch vibrations (e.g., Remmele et al., 1986; McMillan et al., 1993). From multinuclear NMR (^{23}Na,^{27}Al,^{29}Si), Kohn et al. (1989, 1992) concluded, however, that in melt of albite composition there is no evidence for Al-OH or Si-OH bonding but, rather that the principal OH-formation is through interaction with alkalis. Thus, the inference from the NMR data is inconsistent with the assignment of the 900 cm^{-1} band to (Si,Al)-OH stretching. The observation (Mysen and Virgo, 1986a) that the intensity of this band increases continuously with increasing H_2O content (up to 8–10 wt% H_2O) also is inconsistent with an assignment to (Si,Al)-OH. This inconsistency is because in hydrous aluminosilicate glasses with total H_2O content above ~3 wt% results from IR spectroscopy (e.g., Stolper, 1982; Silver and Stolper, 1989; Silver et al., 1990) show that any additional H_2O is dissolved in molecular form. Thus, one would not expect the 900 cm^{-1} band intensity to increase if it was assigned to any kind of vibration associated with structurally bound OH groups. Others have assigned the 900 cm^{-1} band to (Si,Al)-O^- stretching arising from the presence of nonbridging oxygen in the hydrous samples (e.g., Mysen and Virgo, 1986a). Such proposed nonbridging oxygen could be as the result of formation either of M-OH or Al-OH complexes. By forming M-OH complexes, the charge-balance requirement of Al^{3+} in tetrahedral coordination is no longer met. By forming Al-OH complexes, there would be an excess M-cations. In either case, nonbridging oxygen would be formed. (This effect is illustrated with Eqns. 9 and 10 and Table V in Mysen and Virgo, 1986a.) Although clearly more information is needed before the issue can be fully resolved, in the absence of evidence to the contrary, we assign the 900 cm^{-1} band to (Si,Al)-O^- stretching in a depolymerized structural unit (probably of Q^2 type). The spectral interpretation is also consistent with results from anhydrous peralkaline melts and glasses in, for the example, the system Na_2O-Al_2O_3-SiO_2. Spectra of melt and glasses in

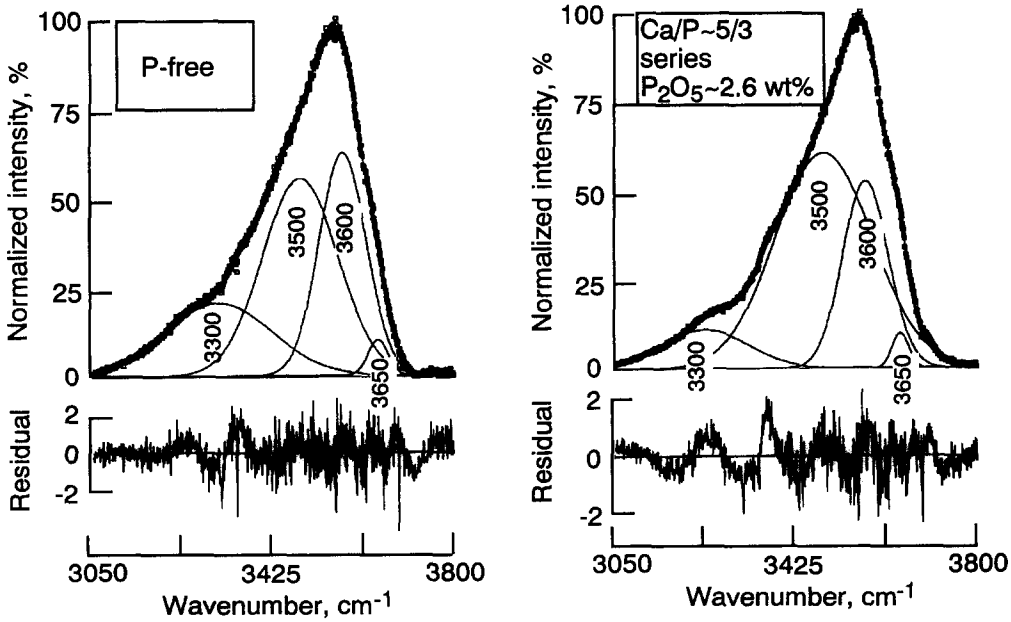

Fig. 7. Examples of curve-fitted spectra in the region of OH stretching.

Table 4. Experimental results—line parameters in the 3000–4000 cm^{-1} region.

		Frequency				Area			
Wt% P_2O_5	A/CNK*	3300	3500	3600	3650	3300	3500	3600	3650
Ca/P~5/3									
0.13	1.05	3316	3484	3572	3644	3152	6086	4305	294
1.11	1.15	3291	3495	3573	3645	2870	7791	3432	257
2.11	1.24	3279	3487	3574	3644	2519	8152	3585	246
2.55	1.34	3245	3488	3573	3644	1406	8605	3512	242
Ca/P~1									
0.15	1.05	3268	3481	3571	3639	2106	8707	3497	210
1.08	1.15	3268	3485	3572	3643	2119	8570	3399	215
2.24	1.24	3256	3471	3572	3644	1953	7936	4348	231
2.86	1.34	3258	3477	3573	3645	1743	7707	4089	256

* Molar $Al_2O_3/(CaO + Na_2O + K_2O)$.

this system reveal significant reduction in frequencies of bands assigned to Si-O^- stretching as the Al/(Al + Si) of the system is increased (Mysen and Frantz, 1994).

The relative intensity of the 900 cm^{-1} band could then be a measure of degree of polymerization of the melts. Interestingly, the area of this band is greater in all the spectra of samples from the Ca/P ~ 1 series. Furthermore, in both series, its relative area decreases somewhat with increasing phosphorus content (Fig. 9). Consequently, one may suggest that in hydrous aluminosilicate melts, P acts as a polymerizing agent analogous to the structural role of phosphorus in anhydrous depolymerized melts (Dupree et al., 1988, 1989; Mysen, 1992). The actual value of NBO/T contributing to the 900 cm^{-1} band intensity may be estimated with the method proposed by Mysen and Virgo (1986a). From such calculations, it would appear that solution of ~9–10 wt% H_2O has increased the NBO/T from near 0 for anhydrous samples to about 0.7 in the hydrous glasses, a value similar to that of trisilicate glasses, for example. There is a 10–25% decrease in this NBO/T-value as phosphorus is dissolved (Table 5).

The Raman band fitted near 970–975 cm^{-1} in the spectra of hydrous glasses, with composition-independent frequency, is assigned to Si-OH stretching (e.g., Stolen and Walrafen, 1976). The presence of Si-OH bonding in these glasses is also consistent with the band near 3650 cm^{-1} in the high-frequency envelope (e.g., Fig. 7, see also Table 4) as OH stretch vibrations at this high frequency has not been associated with hydroxyl formation involving the other metal cations (Al, Ca, Na, K) in the present system (e.g., Aines and Rossman, 1984; Mysen and Virgo, 1986a,b). The dominant intensity in the 3000–4000 cm^{-1} range at lower frequency

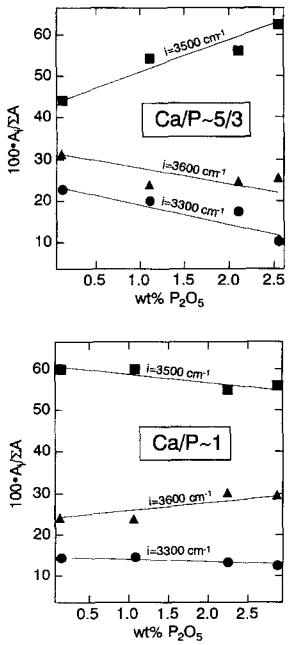

Fig. 8. Variations in areas of individual bands in the OH stretch region relative to the total area of the envelope, ΣA, as a function of wt% P_2O_5 (and A/CNK, see Fig. 1).

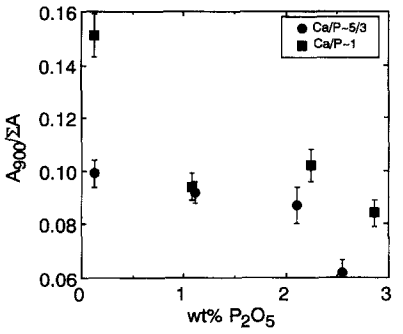

Fig. 9. Relationship between phosphorus content (and A/CNK) the area of the 900 cm^{-1} band (A_{900}) relative to the total area of bands assigned to vibrations not including OH (970 cm^{-1}) and P (1120 and 1210 cm^{-1}). $\Sigma A = A_{900} + A_{1000} + A_{1150} + A_{1200}$.

Table 5. Calculated NBO/T from relative area of 900 cm^{-1} band.

Wt% P_2O_5	A/CNK*	NBO/T ($\pm 1\sigma$)
Ca/P~5/3		
0.13	1.05	0.76 (8)
1.11	1.15	0.59 (6)
2.11	1.24	0.72 (8)
2.55	1.34	0.65 (7)
Ca/P~1		
0.15	1.05	0.74 (8)
1.08	1.15	0.65 (7)
2.24	1.24	0.64 (7)
2.86	1.34	0.65 (7)

* Molar $Al_2O_3/(CaO + Na_2O + K_2O)$.

(e.g., Figs. 7, 8) is consistent with a significant fraction of the OH-groups bonded to metal cations other than Si^{4+} (e.g., Mysen and Virgo, 1986b). This conclusion is also consistent with multinuclear NMR data of hydrous, highly polymerized aluminosilicate melts suggesting primarily alkali-OH interaction (e.g., Kohn et al., 1992).

The three remaining bands in the high-frequency envelope is that near 940–950 cm^{-1} and those near 1120 and 1210 cm^{-1} (Fig. 6). The latter two bands are observed only when there is P in the system. It is suggested that the band fitted near 1120 cm^{-1} might be assigned to P-O-Al stretching thus, in accord with Gan and Hess (1992), leading to the suggestion that phosphate complexing with Al occurs in peraluminous glasses to form perhaps P-O-Al linkages in a three-dimensional structure (see also Mysen et al., 1981).

The band near 1210 cm^{-1} will be interpreted with the aid of published Raman and ^{31}P NMR data (Chakraborty and Condrate, 1985; Kosinski et al., 1988; Dupree et al., 1989). In a vibrational spectroscopic study that included Raman data for Na_2O-SiO_2-P_2O_5 glasses, Chakraborty and Condrate (1985) suggested that a band near 1180 cm^{-1} in their spectra could be assigned to coupled vibrations of Si-O and P-O stretching coordinates. Chakraborty and Condrate (1985) on this basis concluded that this was evidence for Si-O-P linkages in their Na_2O-SiO_2-P_2O_5 glasses. Kosinski et al. (1988) and Dupree et al. (1989) reported ^{31}P NMR evidence for Si-O-P linkages in P-bearing alkali silicate and alkali aluminosilicate glasses. Additionally, Kosinski et al. (1988) suggested that Raman bands in the 1100–1250 cm^{-1} frequency range included vibrations due to Si-O-P linkages. Mysen et al. (1981) in a study of P-bearing $NaAlSi_3O_8$ and $CaAl_2Si_2O_8$ glasses suggested that a band near 1150 cm^{-1} reflected the presence of Si-O-P linkages in those materials. Although somewhat uncertain, we suggest that the band fitted near 1210 cm^{-1} in the spectra of the present glasses also reflects the presence of Si-O-P linkages in the glasses studied here. This suggestion implies structural cross-linking between the phosphate and silicate portion of both the hydrous and anhydrous, peraluminous aluminosilicate glasses.

The area ratio, $A_{1120}/(A_{1120} + A_{1210})$, might be taken as a measure of the relative abundance of P-O-Al and P-O-Si linkages (although this abundance ratio cannot be quantified from the Raman spectra). From the much larger values of $A_{1120}/(A_{1120} + A_{1210})$ in spectra of hydrous as compared with anhydrous samples (Fig. 10) it follows that P-O-Al linkages are more abundant in the hydrous than in the anhydrous P-bearing aluminosilicate glasses.

The 940 cm^{-1} band is significant only in the spectra of hydrous P-bearing samples (Table 3; see also Fig. 6). In these samples, its relative intensity is greater in the series of samples with lowest Ca/P (Table 3). This band could be assigned to $P\text{-}O^-$ stretching in an orthophosphate (PO_4^{3-}) unit (e.g., Nelson and Tallant, 1986; Mysen, 1992). The frequency, however, is about 20 cm^{-1} lower than that observed in many crystalline orthophosphates and also in spectra of other P-bearing glasses where independent spectroscopic evidence indicates that orthophosphate complexes exist (e.g., Nelson and Tallant, 1986; Dupree et al., 1988). Further, Raman spectra of CaO-SiO_2-P_2O_5 and Na_2O-SiO_2-P_2O_5 glasses show the band assigned to $P\text{-}O^-$ stretching in orthosilicate units as a narrow band between 960 and 965 cm^{-1} (Mysen, 1992, 1996). In the present system, with similar metal cations, one would, therefore, expect the frequency to be near 960 cm^{-1} and not 940 cm^{-1} as observed. It should also be noted that despite this inconsistency, if the 940 cm^{-1} band was due to $P\text{-}O^-$ stretching in orthophosphate units in the hydrous samples, from a comparison of the intensity data from the system $Na_2O \cdot 9SiO_2$ (NBO/Si = 0.22) with 2 mol% P_2O_5 in solution with the present intensity relationships, it would be suggested that even in the most P-rich sample, only about 10% of the dissolved P_2O_5 would exist as orthophosphate.

An alternative interpretation may be related to the observation above (e.g., Fig. 10) that the abundance of P-O-Si relative to P-O-Al linkages decreases as H_2O is dissolved in the glasses. This structural change might imply that P-O-Si oxygen bridges have been broken by H_2O. Such breakage could lead to formation of Si-OH and P-OH bonds (analogous to the breakage of Si-O-Si bridges to form two Si-OH bonds in SiO_2-H_2O glasses and melts; see, for example, Wasserburg, 1957; Stolen and Walrafen, 1976). It is possible that the 940 cm^{-1} might be assigned to an equivalent P-OH vibration.

In the study of Mysen and Virgo (1986b), the area of the band near 3500 cm^{-1} was found particularly sensitive to Ca/Si ratio (in spectra of glasses along the join $Ca(OH)_2$-SiO_2), whereas the area of lower-frequency band, near 3300 cm^{-1}, appeared positively correlated with Na/Si (in spectra of glasses along the join NaOH-SiO_2). This latter frequency region also, however, exhibits increased intensity with increasing abundance of molecular H_2O so interpretation of the intensity variations in this region of spectra from the more complex aluminosilicate glasses should be conducted with caution. A band near 3600 cm^{-1} occurred in spectra of glasses along both the joins $Al(OH)_3$-SiO_2 and SiO_2-H_2O (Mysen and Virgo, 1986b). Relative intensity variations re-

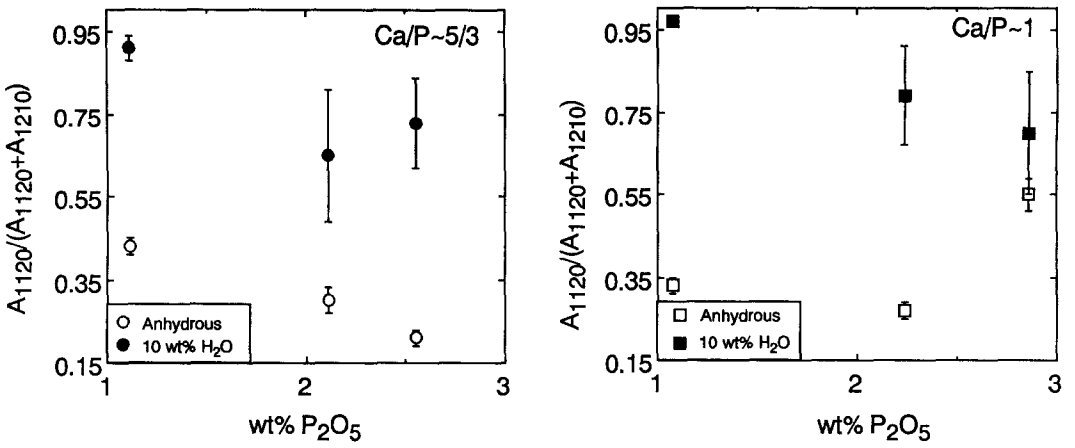

Fig. 10. Relative intensities of the two bands assigned to P-O-Al (A_{1120}) and P-O-Si (A_{1210}) as a function of phosphorus content (and A/CNK) for hydrous (closed symbols) and anhydrous (open symbols) samples.

flecting possible variations in abundance of Al-OH and Si-OH bonding is, therefore, not feasible. It is tentatively suggested, however, that the intensity variations among the 3500 and 3300 cm^{-1} bands (Fig. 8) might reflect relative importance of Ca-OH and alkali-OH bonding. If so, it appears Ca/P ~ 5/3 series with increasing CaO and P_2O_5 content, Ca-OH bonding becomes more important relative to OH groups bonded to alkali metals. In the Ca/P ~ 1 series of glasses, this trend is less evident.

4. DISCUSSION

4.1. Solution Mechanism of Phosphorus in Anhydrous Peraluminous Glasses

The mechanism of incorporation of P in peraluminous glasses is first detailed for the dry compositions. The spectroscopic data are interpreted to suggest that phosphorus is present in the two series of glasses studied primarily as $AlPO_4$ species. There is also evidence for P-O-Si bonding thus suggesting cross-linking between the phosphate complexes and the aluminosilicate network. From Raman spectroscopic data, the presence of phosphate units with double-bonded oxygen can be ruled out (they should appear as peaks at $\geq$1320 cm^{-1}, e.g., Kosinski et al., 1988, and no Raman intensity was observed in this spectral range).

The Al that participates in the formation of $AlPO_4$ units may come from two distinct structural positions. One is where Al^{3+} is charge-balanced with alkalis and possibly Ca. In one case, this mechanism results in the formation of non-bridging oxygen as illustrated with the following schematic equations (for monovalent and divalent charge-balancing cations):

$$2M^{+}AlSi_nO_{2n+2} + P_2O_5 = 2AlPO_4 + 2M^{+}Si_nO_{2n-3} \quad (1)$$

$$M^{2+}Al_2Si_nO_{(2n+4)} + P_2O_5 = 2AlPO_4 + M^{2+}Si_nO_{(2n+1)} \quad (2)$$

Toplis and Dingwell (1996) suggested an alternative mechanism to form $AlPO_4$ complexes where one may envision exchange of alkalies (or alkaline earths) between charge-balanced Al^{3+} and phosphate complexes:

$$M^{+}AlO_2 + P_2O_5 = AlPO_4 + M^{+}PO_3 \quad (1a)$$

$$M^{2+}Al_2O_4 + 2P_2O_5 = 2AlPO_4 + M^{2+}(PO_3)_2 \quad (2a)$$

In the case illustrated by Eqns. 1 and 2, P solution would involve the production of network modifiers (alkalis and Ca), resulting in depolymerization of the melt. This model would have a large influence on the framework structure, which is not observed in the Raman spectra. We, therefore, view this possibility as unlikely. An important implication of this observation is that P incorporation in these aluminosilicate glass systems has little influence on the aluminosilicate network.

Phosphate complexing according to the mechanisms 1a or 2a, or both, does not affect the NBO/T of the aluminosilicate network. However, in this mechanism the Al/(Al + Si) of the aluminosilicate must decrease as phosphorus is dissolved. This postulated decrease in Al/(Al + Si) will result in an increase in frequency of the (Si,Al)-O° stretch vibrations near 1000, 1090, and 1160 cm^{-1} in the P-free glasses (Seifert et al., 1982; Neuville and Mysen, 1996) as P is dissolved. Such a frequency increase is not observed. Further, from a stoichiometric point of view, only metaphosphate (PO_3^-) units can be formed without generating excess Al which might result in additional nonbridging oxygen in the melts. The frequency of P-O$^-$ stretching in PO_3^- units in crystalline $NaPO_3$ is near 1165 cm^{-1} (Nelson and Tallant, 1986). There is no evidence for such a band in the Raman spectra. The mechanisms proposed by Toplis and Dingwell (1996) and illustrated with expressions 1a and 2a are not, therefore, consistent with the data.

An alternative is a conceptually similar model with the phosphate complexes less polymerized than that of PO_3^-. Such a model can be illustrated with the expressions:

$$8M^{+}AlO_2 + 3P_2O_5 = 2AlPO_4 + 2M^{+}4P_2O_7 + 6Al^{3+}(\text{excess}) \quad (1b)$$

$$3M^{+}AlO_2 + P_2O_5 = AlPO_4 + M_3^{+}PO_4 + 2Al^{3+}(\text{excess}) \quad (1c)$$

where Al^{3+}(excess) represents Al^{3+} in excess of that for which alkali charge-compensation would be available. Analogous expressions could be written with divalent cations (e.g., alkaline earths).

Mechanism 1b is unlikely because P-O^- stretching in pyrophosphate units results in Raman bands near 1020 cm^{-1} (Nelson and Tallant, 1985), which have not been observed in the spectra. Mechanism 1c (orthophosphate complexing) will be considered in more detail because there is a very, very weak band near 940 cm^{-1} in the nominally anhydrous samples. By using the Raman data from Mysen (1996) for the purpose of estimating relations between Raman intensity and P concentration, with the $\leq$0.5% of the intensity of the 940 cm^{-1} band relative to the strongest band in the high-frequency envelope of the anhydrous samples, this intensity would correspond to $\leq$0.5% of the total mount of dissolved P_2O_5 in the form of orthophosphate units. It would seem, therefore, that none of the mechanisms involving alkali or alkaline earth exchange between aluminate and phosphate are consistent with the Raman data for these glasses.

In the second possible case, P is structurally bonded with excess Al^{3+} present. This Al^{3+} may be linked either to Si- or Al-bearing Q^3 species, themselves connected to the network. This mechanism is consistent with the phosphorus solubility data of Wolf and London (1994), for example. In that study, it was observed that there was a 1:1 correlation between P solubility and Al content whenever the P/Al = 1. Phosphorus incorporation in such glasses can then be described by the following homogeneous equilibrium:

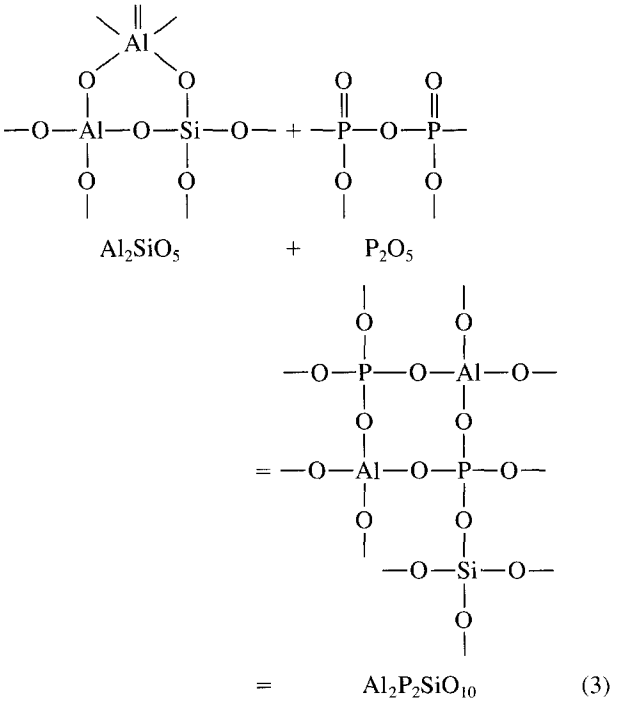

(3)

If some of the original excess Al^{3+} existed in a non-network-forming structural position,[§] the process involves an overall reduction of the NBO/T and the formation of Q^4 species, i.e., polymerization. The Q^4 silicate tetrahedra and charge-balanced AlO_4 tetrahedra forming the network remain unaffected, implying that the structural roles of alkali and Ca do not need to be affected. The total amount of P present in our glasses can be incorporated completely with the above mechanism, because the amount of excess Al^{3+} present exceeds the amount of phosphorus dissolved. This solution mechanism is consistent with the P diffusion data for quite similar bulk compositions in the same system as reported by Wolf and London (1994). Wolf and London (1994) found that there was no absolute or relative change in Na and K concentration in the apatite diffusion aureole compared with the original melt, which is exactly what would be expected from the structural model of P solution proposed here. In other words, the compositions are so Al-rich and peraluminous that there is no need to involve those Al^{3+} atoms charge-balanced by alkalis or Ca^{2+} and forming part of the network (see Table 1).

If, in fact, there is also interaction between P and charge-balanced Al^{3+}, the structural scenario illustrated with Eqns. 1 and 2 requires consideration. Mechanisms 1a,b,c and 2a will not be considered further for the reasons discussed above. In scenarios 1 and 2, nonbridging oxygen will be generated. Relevant Raman bands reflecting increasing depolymerization of the structure as P is dissolved cannot be discerned in the spectra although the sensitivity of the spectra of these samples to such structural features is somewhat difficult to establish quantitatively. A very conservative estimate of the sensitivity might be derived in the following manner. The Raman cross-sections of (Si,Al)-O^- stretch vibrations is on the order of 1 order of magnitude greater than those of (Si,Al)-O° stretching vibrations in these systems (e.g., Mysen, 1995). Therefore, if, for example, a sample contained 5% of structural units containing nonbridging oxygen and 95% fully polymerized units, the Raman intensities from the depolymerized units should be about 50% of the maximum intensity of the high-frequency envelope. This would be easily observed but was not detected in the spectra. A conservative estimate of sensitivity to nonbridging oxygen from this discussion is, therefore, 5% of the total.

4.2. The Role of H_2O in P-Bearing Glasses

The spectroscopic information on hydrous, P-free glasses is consistent with solution of water via association with alkalis or alkaline earths, possibly with Al, and probably with Si. There is also molecular water in the glasses. This conclu-

[§] Al^{3+} without charge-balance in tetrahedral coordination has been suggested to form tri-clusters where Al^{3+} actually also has 4 oxygen ligands (Lacy, 1963). Recently, it has also been suggested that in peraluminous melts, Al^{3+} may reside in structural entities involving four-, five-, and six-fold coordination with oxygen (Sato et al., 1991; Poe et al., 1992). For the present purposes, it is not necessary to know the exact structural position of Al in peraluminous melts other than the fact that the Al is not a part of the aluminosilicate glass and melt network.

sion is consistent with previously suggested models for H_2O solution mechanisms in alumino-silicate melts and glasses (e.g., Mysen and Virgo, 1986b; Silver et al., 1990; Kohn et al., 1992; Holtz et al., 1996).

The Raman spectra of H_2O- and P-bearing glasses differ from both the anhydrous, P-bearing and P-free anhydrous glasses in (1) the presence of a distinct Raman band near 940 cm^{-1} and (2) a considerably larger value of the area ratio, $A_{1120}/(A_{1120} + A_{1210})$ (Fig. 10). The latter observation is consistent with greater relative abundance of P bonded as P-O-Al relative to P-O-Si in hydrous relative to anhydrous P-bearing samples. The relative decline in abundance of Si-O-P bridges in hydrous samples may be due to replacement of the oxygen bridge with OH groups:

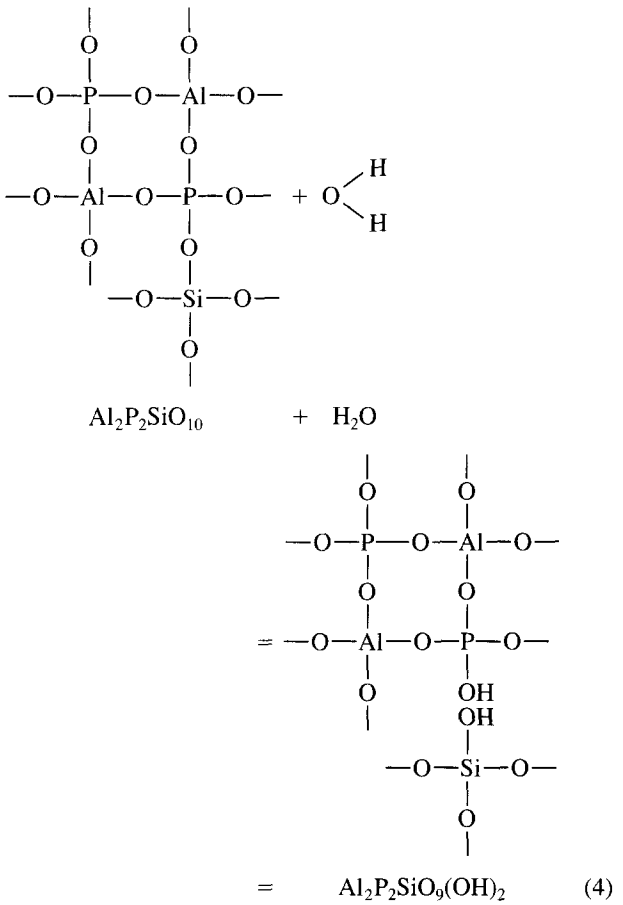

It is possible that the ~940 cm^{-1} band observed in the Raman spectra of hydrous, P-bearing samples might then be assigned to P-OH vibrations analogous to the 970 cm^{-1} that is assigned to Si-OH stretching. Consequently, in this solution model of water into P-bearing peraluminous glasses has the effect of isolating the $AlPO_4$ complexes from the silicate network through the formation of P-OH bonds. A consequence of this solution model for P in hydrous peraluminous glasses is that most likely the solubility of H_2O in P-bearing melts would differ from that in the same melt without phosphorus. Such an effect was demonstrated experimentally by Wolf and London (1994).

5. CONCLUDING REMARKS

Raman spectra of peraluminous granitic glasses are consistent with Al-O-P bonding, perhaps in an $AlPO_4$-type complex, being a principal solution mechanism of P. These complexes are linked with the silicate network over Si-O-P bridges. In hydrous systems, the Si-O-P bridges are broken and replaced with OH-groups attached to Si-OH and probably P-OH. Therefore, the water content of peraluminous aluminosilicate melts are likely to affect the solubility behavior of P, and conversely, the solubility behavior of H_2O is affected by P in such melts.

Acknowledgments—A majority of this work was conducted while one of us (BOM) visited CNRS-CRSCM during the summer of 1994. The hospitality extended by CNRS is greatly appreciated. This work was partially supported by NSF grants EAR9218890 and EAR9614423 to BOM, by a grant from Centre National de la Recherce Scientifique through its Programme International de Cooperation Scientifique (PICS 192) and partially by the NSF-sponsored Center for High-Pressure Research (CHiPR). Critical reviews by M. Toplis, D. London, G. Morgan, and F. R. Ryerson improved the manuscript.

Editorial handling: D. B. Dingwell

REFERENCES

Aines R. D. and Rossman G. R. (1984) Water in minerals? A peak in the infrared. *J. Geophys. Res.* **89,** 4059–4071.

Behrens H. (1995) Determination of water solubilities in high-viscosity melts: An experimental study on $NaAlSi_3O_8$ and $KAlSi_3O_8$ melts. *Eur. J. Mineral.* **7,** 905–920.

Chakraborty I. N. and Condrate R. A. (1985) The vibrational spectra of glasses in the Na_2O-SiO_2-P_2O_5 system with a 1:1 SiO_2:P_2O_5 molar ratio. *Phys. Chem. Glasses* **26,** 68–74.

Davidon W. C. (1966) *Variable Metric Method for Minimization.* Argonne Natl. Lab. ANL 5990.

Dingwell D. B., Knoche R., and Webb S. L. (1993) The effect of P_2O_5 on the viscosity of haplogranite liquids. *Eur. J. Mineral.* **5,** 133–140.

Dupree R., Holland D., and Mortuza M. G. (1988) The role of small amounts of P_2O_5 in the structure of alkali disilicate glasses. *Phys. Chem. Glasses* **29,** 18–21.

Dupree R., Holland D., Mortuza J. A., Collins J. A., and Lockyer M. W. G. (1989) Magic angle spinning NMR of alkali phospho-alumino-silicate glasses. *J. Non-Cryst. Solids* **112,** 111–119.

Galeener F. L. (1982) Planar rings in glasses. *Solid State Comm.* **44,** 1037–1040.

Gan H. and Hess P. C. (1992) Phosphate speciation in potassium aluminosilicate glasses. *Amer. Mineral.* **77,** 495–506.

Hamilton, W. C. (1965) Significance of the crystallographic R-factor. *Acta Cryst.* **18,** 502–510.

Harrison T. M. and Watson E. B. (1984) The behaviour of apatite during crustal anatexis: Equilibrium and kinetic considerations. *Geochim. Cosmochim. Acta* **48,** 1468–1477.

Holtz F., Behrens H., Dingwell D. B., and Johannes W. (1995) H_2O solubility in haplogranitic melts: Compositional, pressure, and temperature dependence. *Amer. Mineral.* **80,** 94–108.

Holtz F., Beny J.-M., Mysen B. O., and Pichavant M. (1996) High-temperature Raman spectroscopy of silicate and aluminosilicate hydrous glasses: Implications for water speciation. *Chem. Geol.* **128,** 25–39.

Kohn S. C., Dupree R., and Smith M. E. (1989) A nuclear magnetic resonance study of the structure of hydrous albite glasses. *Geochim. Cosmochim. Acta* **53,** 2925–2935.

Kohn S. C., Dupree R., and Mortuza M. G. (1992) The interaction between water and aluminosilicate magma. *Chem. Geol.* **96,** 399–410.

Kosinski S. G., Krol D. M., Duncan T. M., Douglass D. C., Mac-

Chesney J. B., and Simpson J. R. (1988) Raman and NMR spectroscopy of SiO_2 glasses co-doped with Al_2O_3 and P_2O_5. *J. Non-Cryst. Solids* **105,** 45–52.

Kushiro I. (1975) On the nature of silicate melt and its significance in magma genesis: Regularities in the shift of the liquidus boundaries involving olivine, pyroxene, and silica minerals. *Amer. J. Sci.* **275,** 411–431.

Lacy E. D. (1963) Aluminum in glasses and melts. *Phys. Chem. Glasses* **4,** 234–238.

London D. (1987) Internal differentiation of rare element pegmatites: Effects of boron, phosphorus and fluorine. *Geochim. Cosmochim. Acta* **51,** 403–420.

London D., Morgan G. B., VI, Babb H. A., and Loomis J. L. (1993) Behavior and effects of phosphorus in the system Na_2O-K_2O-Al_2O_3-SiO_2-P_2O_5-H_2O at 200 MPa (H_2O). *Contrib. Mineral. Petrol.* **113,** 450–465.

Long D. A. (1977) *Raman Spectroscopy.* McGraw-Hill.

Mammone J. F., Sharma S. K., and Nicol M. F. (1981) Ring structures in silica glass—A Raman spectroscopic investigation. *EOS* **62,** 425.

Matson D. W., Sharma S., and Philpotts J. A. (1986) Raman spectra of some tectosilicates and glasses along the orthoclase-anorthite and nepheline-anorthite joins. *Amer. Mineral.* **71,** 694–704.

McMillan P. F., Poe B. T., Stanton T. R., and Remmele R. L. (1993) A Raman spectroscopic study of H/D isotopically substituted hydrous aluminosilicate glasses. *Phys. Chem. Minerals* **19,** 454–459.

Mysen B. O. (1992) Iron and phosphorus in calcium silicate quenched melts. *Chem. Geol.* **98,** 175–202.

Mysen B. O. (1995) Structural behavior of Al^{3+} in silicate melts: In situ, high-temperature measurements as a function of bulk chemical composition. *Geochim. Cosmochim. Acta* **59,** 455–474.

Mysen B. O. (1996) Phosphorus speciation changes across the glass transition in highly polymerized alkali silicate glasses and melts. *Amer. Mineral.* **81,** 1531–1534.

Mysen B. O. and Frantz J. D. (1992) Raman spectroscopy of silicate melts at magmatic temperatures: Na_2O-SiO_2, K_2O-SiO_2, and Li_2O-SiO_2 binary compositions in the temperature range 25–1475°C. *Chem. Geol.* **96,** 321–332.

Mysen B. O. and Frantz J. D. (1994) Structure of haplobasaltic liquids at magmatic temperatures: In situ, high-temperature study of melts on the join $Na_2Si_2O_5$-$Na_2(NaAl)_2O_5$. *Geochim. Cosmochim. Acta* **58,** 1711–1733.

Mysen B. O. and Virgo D. (1986a) Volatiles in silicate melts at high pressure and temperature 2. Water in melts along the join $NaAlO_2$-SiO_2 and a comparison of solubility mechanisms of water and fluorine. *Chem. Geol.* **57,** 333–358.

Mysen B. O. and Virgo D. (1986b) Volatiles in silicate melts at high pressure and temperature. 1. Interaction between OH groups and Si^{4+}, Al^{3+}, Ca^{2+}, Na^+ and H^+. *Chem. Geol.* **57,** 303–331.

Mysen B. O., Virgo D., Harrison W. J., and Scarfe C. M. (1980) Solubility mechanisms of H_2O in silicate melts at high pressures and temperatures: A Raman spectroscopic study. *Amer. Mineral.* **65,** 900–914.

Mysen B. O., Ryerson F. J., and Virgo D. (1981) The structural role of phosphorous in silicate melts. *Amer. Mineral.* **66,** 106–117.

Mysen B. O., Finger L. W., Seifert F. A., and Virgo D. (1982) Curve-fitting of Raman spectra of amorphous materials. *Amer. Mineral.* **67,** 686–696.

Nelson C. and Tallant D. R. (1984) Raman studies of sodium silicate glasses with low phosphate contents. *Phys. Chem. Glasses* **25,** 31–39.

Nelson C. and Tallant D. R. (1986) Raman studies of sodium phosphates with low silica contents. *Phys. Chem. Glasses* **26,** 119–122.

Neuville D. R. and Mysen B. O. (1996) Role of aluminum in the silicate network: In situ, high-temperature study of glasses and melts on the join SiO_2-$NaAlO_2$. *Geochim. Cosmochim. Acta* **60,** 1727–1738.

Pichavant M. (1987) Effects of B and H_2O on liquidus phase relations in the haplogranite system. *Amer. Mineral.* **72,** 1056–170.

Pichavant M., Montel J.-M., and Richard L. (1992) Apatite solubility in peraluminous liquids: Experimental data and an extension of the Harrison-Watson model. *Geochim. Cosmochim. Acta* **56,** 3855–3861.

Poe B. T., McMillan P. F., Cote B., Massiot D., and Coutoures J.-P. (1992) SiO_2-Al_2O_3 liquids: In situ study by high-temperature ^{27}Al NMR spectroscopy and molecular dynamics simulations. *J. Phys. Chem.* **96,** 8220–8224.

Remmele R., Stanton T., McMillan P. F., and Holloway J. R. (1986) Raman spectra of hydrous glasses along the quartz-albite join. *EOS* **67,** 1274.

Revesz A. G. and Walrafen G. E. (1983) Structural interpretation of some of the Raman lines from vitreous silica. *J. Non-Cryst. Solids* **54,** 323–355.

Richard L. R., Pichavant M., Clarke D. B., and Montel J.-M. (1992) Effects of temperature, composition, and $f\,O_2$ on apatite solubility and phosphorus behaviour in peraluminous granitic melts. V. M. Goldschmidt Conf., Reston, A-90. (abstr.)

Roux J., Holtz F., Lefevre A., and Schulze F. (1994) A reliable high-temperature setup for internally-heated pressure vessels: Application to silicate melt studies. *Amer. Mineral.* **79,** 1145–1150.

Ryerson F. J. and Hess P. C. (1980) The role of P_2O_5 in silicate melts. *Geochim. Cosmochim. Acta* **44,** 611–624.

Sato R. K., McMillan P. F., Dennison P., and Dupree R. (1991) A structural investigation of high alumina glasses in the CaO-Al_2O_3-SiO_2 system via Raman and magic angle spinning nuclear magnetic resonance spectroscopy. *Phys. Chem. Glasses* **32,** 149–160.

Seifert F. A., Mysen B. O., and Virgo D. (1982) Three-dimensional network structure in the systems SiO_2-$NaAlO_2$, SiO_2-$CaAl_2O_4$, and SiO_2-$MgAl_2O_4$. *Amer. Mineral.* **67,** 696–711.

Seifert F. A., Mysen B. O., and Virgo D. (1983) Raman study of densified vitreous silica. *Phys. Chem. Glasses* **24,** 141–145.

Silver L. and Stolper E. (1989) Water in albitic glasses. *J. Petrol.* **30,** 667–710.

Silver L., Ihinger P. D., and Stolper E. (1990) The influence of bulk composition on the speciation of water in silicate glasses. *Contrib. Mineral. Petrol.* **104,** 142–162.

Stolen R. H. and Walrafen G. E. (1976) Water and its relation to broken bond defects in fused silica. *J. Chem. Phys.* **64,** 2623–2631.

Stolper E. (1982) The speciation of water in silicate melts. *Geochim. Cosmochim. Acta* **46,** 2609–2620.

Toplis M. J. and Dingwell D. W. (1996) The variable influence of P_2O_5 on the viscosity of melts of differing alkali/aluminum ratio: Implications for the structural role of phosphorus insilicate melts. *Geochim. Cosmochim. Acta* **60,** 4107–4121.

Toplis M. J., Dingwell D. B., and Libourel G. (1994a) The effect of phosphorus on the iron redox ratio, viscosity, and density of an evolved ferro-basalt. *Contrib. Mineral. Petrol.* **117,** 293–304.

Toplis M. J., Libourel G., and Carroll M. R. (1994b) The role of phosphorus in crystallization processes of basalt: an experimental study. *Geochim. Cosmochim. Acta* **58,** 797–810.

Vielzeuf D. and Montel J. M. (1994) Partial melting of metagreywackes. Part I. Fluid-absent experiments and phase relationships. *Contrib. Mineral. Petrol.* **117,** 375–393.

Visser W. and Koster Van Groos A. F. (1979) Effects of P_2O_5 and TiO_2 on liquid-liquid equilibria in the system K_2O-FeO-Al_2O_3-SiO_2. *Amer. J. Sci.* **279,** 970–988.

Wasserburg G. J. (1957) The effects of H_2O in silicate systems. *J. Geol.* **65,** 15–23.

Watson E. B. (1976) Two-liquid partition coefficients: experimental data and geochemical applications. *Contrib. Mineral. Petrol.* **56,** 119–134.

Watson E. B. and Capobianco C. J. (1981) Phosphorus and the rare-earth elements in felsic magmas: an assessment of the role of apatite. *Geochim. Cosmochim. Acta* **45,** 2349–2358.

Wolf M. B. and London D. (1994) Apatite dissolution into peraluminous granitic liquids: An experimental study of solubilities and mechanisms. *Geochim. Cosmochim. Acta* **58,** 4127–4145.

Wyllie P. J. and Tuttle O. F. (1964) Experimental investigation of silicate systems containing two volatile components. III. The effects of SO_3, P_2O_5, HCl, and Li_2O in addition to H_2O on the melting temperatures of albite and granite. *Amer. J. Sci.* **262,** 930–939.